Journal of Hydraulic Research

ISSN: 0022-1686 (Print) 1814-2079 (Online) Journal homepage: http://www.tandfonline.com/loi/tjhr20

Modelling deltaic progradation constrained by a moving sediment source

Hsi-Heng Dai , Rocío Luz Fernandez , Gary Parker , Marcelo H. Garcia & Wonsuck Kim

To cite this article: Hsi-Heng Dai , Rocío Luz Fernandez , Gary Parker , Marcelo H. Garcia & Wonsuck Kim (2013) Modelling deltaic progradation constrained by a moving sediment source, Journal of Hydraulic Research, 51:3, 284-292, DOI: 10.1080/00221686.2012.762554

To link to this article: http://dx.doi.org/10.1080/00221686.2012.762554

Journal of Hydraulic Research Vol. 51, No. 3 (2013), pp. 284–292
http://dx.doi.org/10.1080/00221686.2012.762554

Research paper

Modelling deltaic progradation constrained by a moving sediment source

HSI-HENG DAI, Associate Professor, *Department of Water Resources and Environmental Engineering, Tamkang University, Taipei County, Taiwan.*
Email: hdai@mail.tku.edu.tw

ROCÍO LUZ FERNANDEZ, Researcher, *National Scientific and Technical Research Council (CONICET), Universidad Nacional de Córdoba, Cordoba 5016, Argentina.*
Email: rocioluz@efn.uncor.edu (author for correspondence)

GARY PARKER (IAHR Member), Professor, *Department of Civil and Environmental Engineering and Geology, University of Illinois at Urbana-Champaign, Urbana, IL 61801, USA.*
Email: parkerg@illinois.edu

MARCELO H. GARCIA (IAHR Member), Professor, *Hydrosystems Laboratory, Department of Civil and Environmental Engineering, University of Illinois at Urbana-Champaign, Urbana, IL 61801, USA.*
Email: mhgarcia@illinois.edu

WONSUCK KIM, Assistant Professor, *Department of Geological Sciences, Jackson School of Geosciences, University of Texas at Austin, Austin, TX 78712-0254, USA.*
Email: delta@jsg.utexas.edu

ABSTRACT
A physically-based moving boundary model of deltaic progradation is developed. Surface of the axially symmetric, inner delta is free to grow or shrink in time, while the sediment source is allowed to migrate along the streamwise direction. Particularly, the model developed here captures the control of a downstream migrating sediment source on a lateral extent of the delta. Along this line, the modelling results provide insight into the sedimentation processes associated with elongated fan–delta systems. Further calculations allow to determining the influence of ratio between water and sediment discharges on delta morphology. The model uses appropriately the laboratory observations described in a companion paper.

Keywords: Delta; numerical model; progradation; sediment transport; tailing; turbidity current

1 Introduction

Formally, a delta can be defined as a coastal sedimentary deposit with both subaerial and subaqueous parts. Hence, a delta displays commonly a low-slope, fluvially-deposited topset, a high-slope, coarse-grained foreset which progrades by grain avalanching, and a low-slope bottomset deposit that forms as the fines settle out on the bed of the water body (Graf 1971, Swenson *et al.* 2000, Kostic and Parker 2003a, Garcia 2008, Gerber *et al.* 2008). Early efforts on fluvial fan-shaped modelling, characterized by a radially symmetric geometry, have been focused on a fixed source of sediment (Whipple *et al.* 1998, Sun *et al.* 2002, Kostic and Parker 2003b, and others). Under upstream fixed source configurations, either the sediment feed point aggrades with time (Parker *et al.* 1998) or the size of the fan–delta grows radially (Kostic and Parker et al. 1998a, 1998b). By contrast, if the feeding point for sediment and water is allowed to migrate downstream, the laboratory observations by Fernandez *et al.* (2011) have recently shown that under the appropriate source moving conditions, the fan–delta does not fill the available space in standing water as it progradates. Instead, it forms a lengthened depositional system.

The present study involves the development of a numerical inner delta model that describes the co-evolution of the prograding topset and foreset face deposits under the condition of a

Revision received 12 June 2012/Open for discussion until 30 November 2013.

ISSN 0022-1686 print/ISSN 1814-2079 online
http://www.tandfonline.com

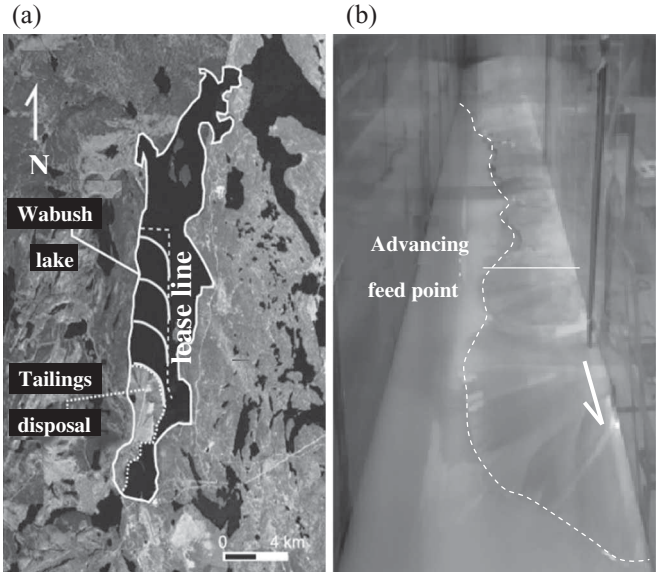

Figure 1 (a) Aerial view of Wabush Lake showing the elongated sub-aerial fan-tailing deposit extended northward from the western side of the lake. The lease line and expected future pattern of progradation are also indicated. (b) Top view of laboratory fan–delta after successive downstream relocations of feed point (Fernandez *et al.* 2011)

moving sediment source. Such a challenge is motivated by an effort to optimize the management and lengthen the lifetime of the tailings basin of a mine in Wabush Lake, Canada (Fig. 1a). The optimal use of the tailings requires that it should be managed so that tailings are effectively disposed with the most effective storage consistent with environmental restrictions. Thus, the leased zone permitted to be used by the mining company is about 2 km in width and 8 km in length. To maintain tailings within the leased area, it is then necessary to move the slurry pipelines, resulting in the development of an elongated fan–delta as shown in Fig. 1a for field conditions. Figure 1b shows the laboratory work reported in Fernandez *et al.* (2011), which is used to validate the numerical approach described here. Under the laboratory conditions, the downstream migration of feed point was used to limit the lateral extent of the prograding deposit, so leaving unfilled open water on one side (Fig. 1b). This article deals with the modelling of the dynamics that lead to such a delta configuration, which also could find its natural counterpart in the morphology of the birdfoot delta of the Mississippi River, where the leveed channel serves as the moving slurry pipeline (Kim *et al.* 2009).

The formulation reported here assumes that sedimentation occurs only upstream of the delta toe, so that the formation of the low-slope bottomset of the deposit is not being modelled.

2 Modelling approach

2.1 *Moving coordinate system*

The fluvial zone, located upstream of the top of the foreset, exhibits commonly a conical shape (Hooke and Rohrer 1979) and it is thus approximated here as axially symmetric, as shown

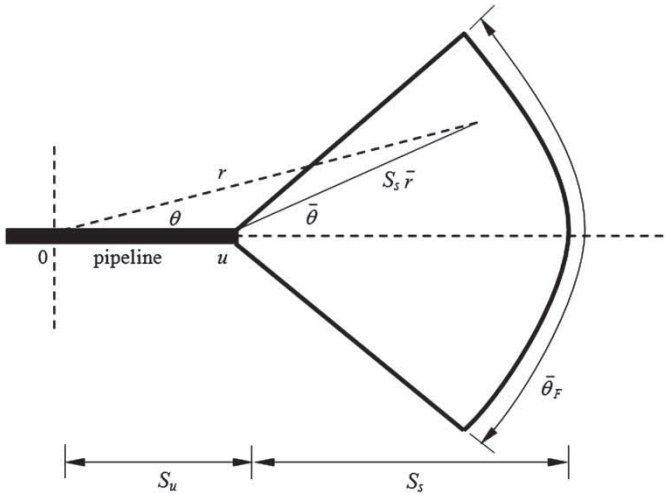

Figure 2 Definition sketch for the plan view of the axially symmetric alluvial fan and coordinate system used in the formulation. The pipeline is delivering sediment through point "*u*" and moving downstream of the delta topset

in Fig. 2. The fan–delta expands an angle of $\bar{\theta}_F$ and its shoreline is at the distance S_s from the mobile feed point. The sediment source is at the vertex of the fan–delta, and it is denoted by "*u*" in Fig. 2. With time, the sediment source point moves downstream at a constant elevation. Regarding the fan–delta surface, it may grow or shrink in size; therefore, S_u and S_s are continuous functions of time.

Since both the sediment source point and the shoreline position are able to move, it is appropriate to use a transformation to map the spatial domain on the fan–delta, $0 \le r \le S_s$, into the finite interval, $\bar{r} \in [0, 1]$, via $\bar{r} = r/S_s$, where the feed point is at $\bar{r} = 0$ and the shoreline is at $\bar{r} = 1$. Therefore, two coordinate systems are established: (a) r, θ, and t: they refer to the fixed coordinates (dashed lines in Fig. 2) and (b) $\bar{r}$, $\bar{\theta}$, and $\bar{t}$: they refer to the transformed coordinates which are moving with the fluvial delta. Hereafter, $(-)$ denotes quantities in the transformed (moving) coordinates. In particular, r is the dimensional radius of the fan–delta, while $\bar{r}$ is the dimensionless counterpart. Other quantities, such as t, $\bar{t}$, S_u, and S_s remain dimensional throughout the derivation.

The two coordinate systems are then shifted spatially by a distance S_u, and an arbitrary point on the active fan can be written in terms of both coordinate systems:

$$S_s\bar{r}\cos\bar{\theta} + S_u = r\cos\theta \tag{1}$$

$$S_s\bar{r}\sin\bar{\theta} = r\sin\theta \tag{2}$$

$$\bar{t} = t \tag{3}$$

$$\bar{\theta} = \tan^{-1}\left(\frac{r\sin\theta}{r\cos\theta - S_u}\right) \tag{4}$$

Without loss of generality, it is assumed that $S_s \gg S_u$ and the temporal and spatial derivatives give the following expressions,

respectively,

$$\frac{\partial}{\partial t} = \frac{\partial}{\partial t} - \frac{\cos\bar{\theta}\dot{S}_u + \bar{r}\dot{S}_s}{S_s}\frac{\delta}{\partial \bar{r}} + \frac{\dot{S}_u \sin\bar{\theta}}{S_s \bar{r}}\frac{\partial}{\partial \bar{\theta}} \tag{5}$$

$$\frac{\partial}{\partial r} = \frac{1}{S_s}\frac{\partial}{\partial \bar{r}} \tag{6}$$

$$\frac{\partial}{\partial \theta} = \frac{\partial}{\partial \bar{\theta}} \tag{7}$$

where t refers time. As the fan–delta moves, $-\bar{\theta}_F/2 \le \bar{\theta} \le \bar{\theta}_F/2$ and $0 \le \bar{r} \le 1$. The sediment source point moves with speed $\dot{S}_u$ and the fan–delta is growing/shrinking at a rate $\dot{S}_s$. Both $\dot{S}_u$ and $\dot{S}_s$ are also general functions of time, in which $(\dot{})$ represents the time rate of change.

2.2 *Moving coordinate system*

The governing equation employed here is the Exner equation, which in the fixed coordinates and by assuming no migration of the feed point, it can be written as

$$(1-\lambda_p)\frac{\partial \eta}{\partial t} = -\frac{1}{r}\frac{\partial r q_r 1}{\partial r} - \frac{1}{r}\frac{\partial q_\theta}{\partial \theta} \tag{8}$$

where λ_p is the porosity of the deposit, η is the elevation of the deposit surface at any point on the fan–delta, and q_r and q_θ are the sediment transport rates in the radial and azimuthal directions, respectively. Since the active channels continuously rework across the fan–delta region, provided the time scale in our formulation is sufficiently long compared with the avulsion time scale of the active channels, in a statistical sense we may assume that the sediment transport rate is only in the radial direction, while it is assumed to be negligible along the azimuthal direction. With the assumption of axial symmetry, η and q_r, are functions of r only, and the Exner equation in the transformed coordinates can be written as

$$(1-\lambda_p)\left(\frac{\partial \eta}{\partial t} - \frac{\cos\bar{\theta}\dot{S}_u + \bar{r}\dot{S}_s}{S_s}\frac{\partial \eta}{\partial \bar{r}}\right) = -\frac{1}{S_s \bar{r}}\frac{\partial \bar{r} q_{\bar{r}}}{\partial \bar{r}} \tag{9}$$

Here, the transformed spatial domain is $\bar{r} \in [0,1]$ and $\bar{\theta} \in [-\bar{\theta}_F/2, \bar{\theta}_F/2]$, where $\bar{\theta}_F$ is the angle at which fan–delta expands, as it was defined earlier. By integrating the above equation with respect to $\bar{\theta}$ over $-\bar{\theta}_F/2 \le \bar{\theta} \le \bar{\theta}_F/2$, it results

$$\frac{\partial \eta}{\partial t} = \frac{2\dot{S}_u \sin(\bar{\theta}_F/2) + \bar{r}\bar{\theta}_F \dot{S}_s}{S_S \bar{\theta}_F}\frac{\partial \eta}{\partial \bar{r}} - \frac{1}{(1-\lambda_p)S_s^2 \bar{\theta}_F \bar{r}}\frac{\partial Q_t}{\partial \bar{r}} \tag{10}$$

where $Q_t = S_s \bar{r}\bar{\theta}_F q_{\bar{r}}$ is the total sediment transport rate across an arc over the entire fan–delta.

2.3 *Sediment feed condition*

Since the sediment feed is maintained at a constant rate, the Exner equation at the sediment source point is used then to set-up a relation for its moving speed $\dot{S}_u$, which is termed here as the feed point condition. To avoid the singularity existing at the vertex of the active fan–delta, where $\bar{r} \to 0$, the Exner equation is evaluated at the grid nearest to the vertex, that is, $\bar{r} = \Delta\bar{r}$. This condition also implies that the sediment is delivered into the fan–delta system through a finite opening width. The Exner equation evaluated at $\bar{r} = \Delta\bar{r}$ is then

$$(1-\lambda_p)\left(2\dot{S}_u \sin\left(\frac{\bar{\theta}_F}{2}\right) + \bar{\theta}_F \dot{S}_s \Delta\bar{r}\right)\frac{\partial \eta}{\partial \bar{r}_{\bar{r}=\Delta\bar{r}}} = \frac{1}{S_s \Delta\bar{r}}\frac{\partial Q_t}{\partial \bar{r}_{\bar{r}=\Delta\bar{r}}} \tag{11}$$

2.4 *Shock and shoreline conditions*

The shock condition at the foreset allows this delta-face to prograde by placing all of the sediment delivered from the fluvial topset to the foreset, so that, the foreset slope S_a is maintained constant, being deposited via frequent avalanching. This condition is obtained by integrating the Exner equation for sediment continuity over the foreset (see below).

Figure 3a shows a sketch for the sectional view of the fan–delta as considered in the formulations, while the laboratory progradation at a constant foreset slope is illustrated by Fig. 3b, based on the experimental observations reported in Fernandez *et al.* (2011).

The flow on the fluvial delta is assumed to be sufficiently thin so that at the shoreline, the fluvial surface has the same elevation as the water level, which here it is assumed to be steady as waves and water levels variations are insignificant in Wabush Lake. The shoreline and the toe of the foreset are S_s and S_b away from the vertex of the active part of the fan–delta, respectively. Then,

$$S_b - S_s = \frac{\eta_{\bar{r}=1} - \eta_{bu} - X_b S_s \cos\bar{\theta}}{S_a - X_b \cos\bar{\theta}} \tag{12}$$

where $\eta_{\bar{r}=1}$ refers to the shoreline elevation, η_{bu} is the base elevation at the feed point, andX_b is the base slope. Considering a horizontal base, that is, $X_b = 0$, leads to the following simplified equation:

$$S_b - S_s = \frac{\Delta\eta_f}{S_a} \tag{13}$$

in which $\Delta\eta_f = \eta_{\bar{r}=1} - \eta_{bu}$ is the elevation drop from the shoreline to the toe on the foreset.

We may now double integrate the Exner's equation over $1 \le \bar{r} \le S_b/S_s$ and $-\bar{\theta}_F/2 \le \bar{\theta} \le \bar{\theta}_F/2$. It is assumed that no sediment escapes from the foreset, so the shoreline condition, that is, shock condition, is derived as

$$Q_{ts} = \frac{1}{2}(1-\lambda_p)S_a\left(\dot{S}_s\bar{\theta}_F + 2\dot{S}_u \sin\frac{\bar{\theta}_F}{2}\right) \times \left[2S_s\frac{\Delta\eta_f}{S_a} + \left(\frac{\Delta\eta_f}{S_a}\right)^2\right] \tag{14}$$

in which Q_{ts} is the total sediment transport rate along the shoreline.

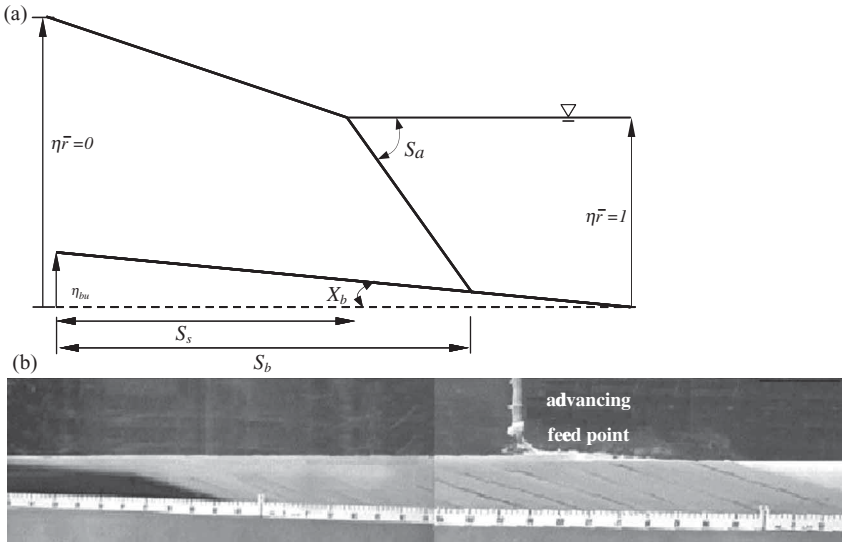

Figure 3 (a) Side view of the fan–delta. The view is taken from a slice at $\bar{\theta} = 0$, X_b is the base slope, and S_a is the foreset slope. The sediment feed point is at the level $\eta_{\bar{r}=0}$, while the shoreline is at the level $\eta_{\bar{r}=1}$. The shoreline and the toe of the foreset are S_s and S_b away from the sediment source point, respectively. (b) Delta progradation showing evolution details of constant sloping topset and foreset faces. The view is from left tank side, scale in centimeter

2.5 *Continuity condition at the foreset*

The point where the foreset joins the base, it provides the relation for the moving speed of the foreset toe, that is, $\dot{S}_b$. This termed the continuity condition approximated by

$$\eta_{\bar{r}=1} - S_a(S_b - S_s) = \eta_{\text{bu}} - S_b X_b \cos\bar{\theta} \tag{15}$$

After taking the time derivative, it gives

$$\dot{S}_b = \frac{S_a\dot{S}_s + X_b\dot{S}_u}{S_a - X_b\cos\bar{\theta}} \tag{16}$$

For the case of horizontal base, that is, $X_b = 0$, the continuity condition simplifies to $\dot{S}_b = \dot{S}_s$.

2.6 *Internal relations*

Further progress on solving the fan–delta morphodynamics relies on the relations that describe the flow and sediment transport processes within the channels along the topset deposit. To be consistent with field observations (Locat *et al.* 2007) and laboratory results (Fernandez *et al.* 2011), the model assumes here that the delta is built by frequent avulsions and reworking of surface by active fluvial channels. Particularly, as the sediment grain size deposited on the fan–delta is considered to be in the range of sand (Fernandez *et al.* 2011), the present study includes the development of internal relations for the transport rate of sand in the radial direction, q_r.

A set of laboratory experiments is thus performed to only focus on measuring both the sediment transport and resistance relationships. The resulting expressions of this experimental data are then introduced into the numerical model to simulate the sediment transport on the fluvial-fan in the tailings modelling laboratory experiments performed by Fernandez *et al.* (2011). The experiments that allowed the transport relationships were conducted in a small, narrow acrylic-sided flume (0.05 m wide, 1 m long, and 0.25 m deep) specially designed for the study of sediment transport. A peristaltic pump delivered slurry at a known discharge into the small flume to its upstream end, as shown in Fig. 4a. Outflowing sediment was captured at the downstream and weighed to determine sediment transport rates. Only model "sand" ($d_{50} = 30\,\mu$m) was used in these experiments.

In the course of the 24 experiments that were performed, water discharges were varied within the range of 200–1200 ml min^{-1}, while volume sediment inflow concentrations ranged from 2 to 17%; being water and sediment discharges held constant for a given experiment. Each experiment was commenced with a bare, horizontal bottom. With time, the bed aggraded to equilibrium with a slope in grade with the water and sediment discharges (Fig. 4b). Once equilibrium was reached, flow depth, h, and bed slope, S were measured. Weighing of successive samples of the sediment captured downstream under equilibrium conditions allowed the determination of the sediment transport rate at equilibrium.

Thus, letting q_r denote the volume sediment transport rate per unit width, Fig. 5a shows its dimensionless form, $q_r^* = q_r/(\sqrt{Rgd_{50}}d_{50})$ as a function of the dimensionless shear stress, $\tau^* = hS/(Rd_{50})$, where R is the submerged specific gravity of the sediment ($\sim$1.65 for quartz). The best-fit regression line is given by $q_r^* = 0.21\tau^{*2.71}$, with a multiple correlation coefficient, $r^2 = 0.867$.

Flow resistance relation. Regarding data on flow resistance, Fig. 5b shows the bed drag coefficient, C_f, as a function of the Reynolds number, R. Here, $\mathsf{R} = Ud_{50}/\upsilon$, in which U denotes the mean flow velocity and υ, the kinematic viscosity assumed

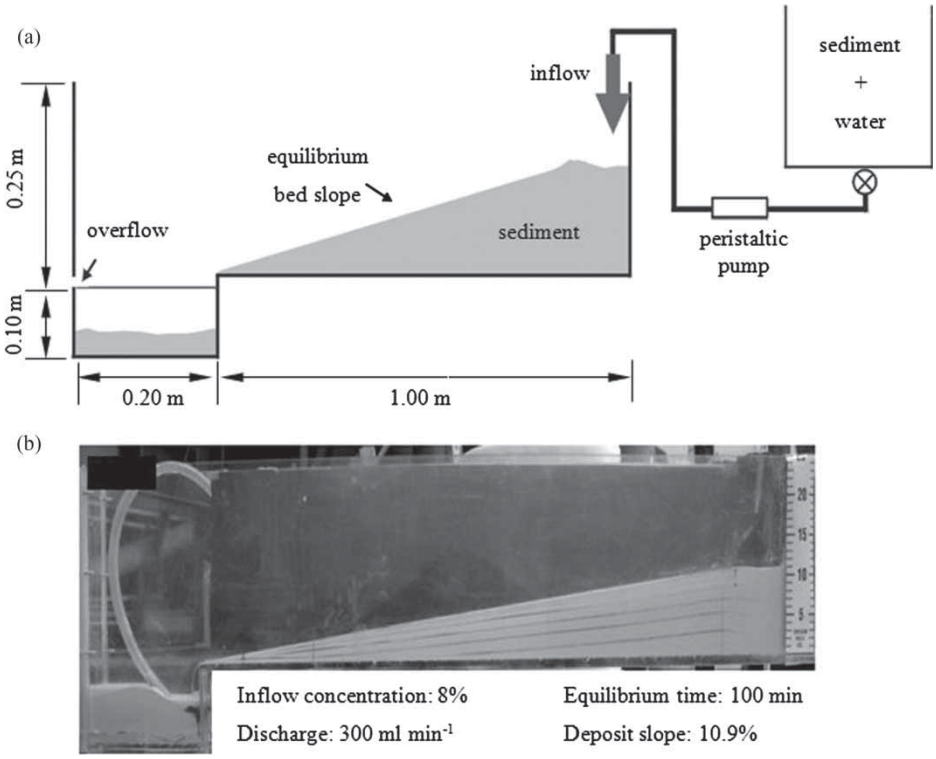

Figure 4 (a) Sketch of the experimental facilities for the sediment transport experiments. (b) Photograph showing the equilibrium depositional slope reached in one of the experiments

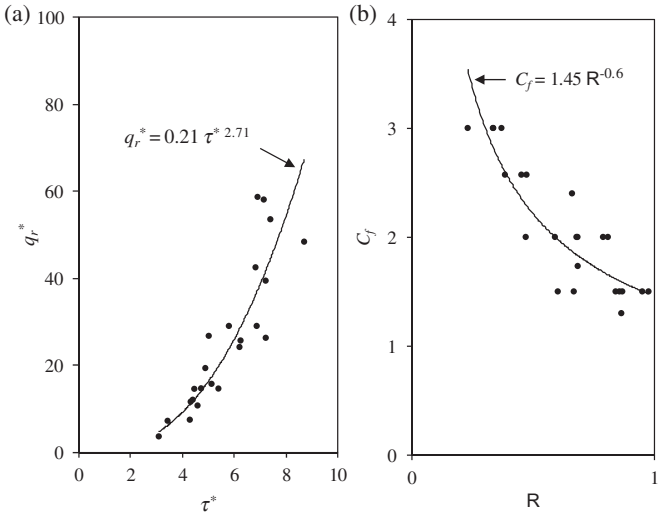

Figure 5 (a) Sediment transport relation resulted from the experiments. (b) Friction factors determined from flow depth, slope, and velocity data, plotted against Reynolds numbers

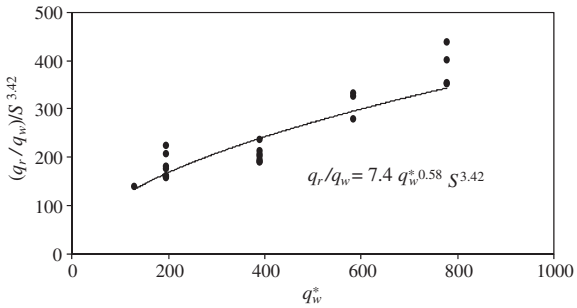

Figure 6 Ratio $(q_r/q_w)/S^{3.42}$ versus q_w^* from the sediment transport experiments

$1 \times 10^{-6}\,\mathrm{m^2\,s^{-1}}$. The best-fit regression line for this data was $C_f = 1.45\mathrm{R}^{-0.6}$ with $r^2 = 0.752$.

Data reduction for sediment transport relation. Subsequent analysis by sorting the data of Fig. 5a according to the different flow rates yields a stronger dependence of S on the ratio q_r/q_w with a value for the exponent that increased from 1.67 to a mean value of 3.42, as indicated by Fig. 6. Here, q_w refers to the water supply rate per unit width. Therefore, the sediment transport relation could alternatively be cast in terms of the flow discharge and bed slope in the following simple form:

$$\frac{q_r}{q_w} = 7.4\, q_w^{*0.58} S^{3.42} \tag{17}$$

according to the data regression of Fig. 6. In Eq. (17) $q_w^* = q_w/(\sqrt{gd_{50}}d_{50})$. As in the Engelund–Hansen expression (1967), Eq. (17) does not include any kind of critical value for the initiation of sediment transport, but it can be used to compute material load that is within the range of the diameter used in the laboratory (i.e. $\sim$10 μm).

The above relationships developed by considering similitude rules were then incorporated into the numerical model for the computation of the sediment transport on the fluvial part of the fan–delta deposit. The total transport rate is then $Q_t = B_{\mathrm{ac}} q_r$,

where B_{ac} refers to the total width of active channels calculated based on the conservation of mass, $B_{ac} = Q_w S/(URd_{50}\tau)^*$.

3 Steady-state solution: a permanent form

Based on the experimental observations detailed on the companion paper (Fernandez *et al.* 2011) and as suggested by Fig. 4b, the fan–delta system approaches to a steady state (with a permanent form) as it propagates downstream over a flat basement. Hence, as the sediment feed point moves downstream and the fan builds outward, there exists a permanent form solution on a horizontal base in which $\dot{S}_s = 0$, and the fan–delta system migrates downstream with a constant speed $\dot{S}_u$. Physically, this permanent form solution represents a dynamic equilibrium between the sediment input rate and the progradation of the fan–delta system which is moving forward with a constant speed without varying its geometry.

In the reference frame moving with the fan–delta, the system is in a steady state, that is, $\partial/\partial\bar{t} = 0$. Dropping the time-dependence term in the Exner expression, Eq. (9) reduces to the form

$$(1-\lambda_p)\cos\bar{\theta}\dot{S}_u\frac{\partial\eta}{\partial\bar{r}} = \frac{1}{\bar{r}}\frac{\partial\bar{r}q_{\bar{r}}}{\partial\bar{r}} \tag{18}$$

Equation (18) can be integrated over $\bar{\theta} \in [-\bar{\theta}_F/2, \bar{\theta}_F/2]$ and $\bar{r} \in [0, \bar{r}]$

$$Q_t = Q_0 + 2(1-\lambda_p)S_s\dot{S}_u\sin\frac{\bar{\theta}_F}{2}\left[\bar{r}\eta - \int_0^{\bar{r}}\eta\,\mathrm{d}p\right] \tag{19}$$

in which $Q_t = S_s\bar{r}\bar{\theta}_F q_{\bar{r}}$ and Q_0 is the sediment feed rate. At the shoreline ($\bar{r} = 1$), the total sediment transport rate is given by

$$Q_{ts} = Q_0 + 2(1-\lambda_p)S_s\dot{S}_u\sin\frac{\bar{\theta}_F}{2}\left[\eta_{\bar{r}=1} - \int_0^{1}\eta\,\mathrm{d}p\right] \tag{20}$$

Since $\dot{S}_s = 0$ in the permanent form solution, the whole fan–delta moves downstream with the same speed $\dot{S}_u$. Using the shock condition mentioned earlier, $S_b - S_s = \Delta\eta_f/S_a$, Eq. (20) is written in the form

$$\dot{S}_u = \frac{Q_{ts}}{\begin{array}{l}[2(1-\lambda_p)S_s\Delta\eta_f\sin(\bar{\theta}_F/2) \\ \quad + (\Delta\eta_{f^2}/S_a)(1-\lambda_p)\sin(\bar{\theta}_F/2)]\end{array}} \tag{21}$$

where $\Delta\eta_f$ is the elevation drop from the shoreline to the base. Therefore, Eq. (21) yields

$$\dot{S}_u = \frac{Q_0}{\begin{array}{l}(1-\lambda_p)\sin(\bar{\theta}_F/2)[2S_s\Delta\eta_f] \\ \quad + \Delta\eta_{f^2}/S_a - 2S_s(\eta_{\bar{r}=1}\int_0^1\eta\,\mathrm{d}p)\end{array}} \tag{22}$$

and the following expression is obtained by solving for Q_t

$$Q_t = Q_0\left[1 + D\left(\bar{r}\eta - \int_0^{\bar{r}}\eta\,\mathrm{d}p\right)\right] \tag{23}$$

where $D = 2S_s/[2S_s\Delta\eta_f + \Delta\eta_{f^2}/S_a - 2S_s(\eta_{\bar{r}=1} = \int_0^1\eta\,\mathrm{d}p)]$. Note that the fan–delta surface elevation, η, and its size, S_s, are not known *a priori*. The above equations need to be solved iteratively until a convergent solution is reached.

4 Application to Wabush tailings: permanent form solution

For the situation described here, the parameters related to the tailings basin in Wabush Lake are adopted. The fan–delta currently has a radius of approximately 1470 m and an expanding angle of 120°. The specific gravity of the tailings discharged to the fan–delta is about 3.05. The porosity of the deposited sediment, λ_p, is approximately 0.4 (Fernandez *et al.* 2011). Other *in situ* parameters are listed in Table 1, which are based on the condition at the field at the moment of this work. However, the tailings production rate, Q_0, and the water supply rate, Q_w, could change with time. The focus of this section is to investigate the influence of doubling the tailings production rate (Case 1) and the influence of doubling the water supply rate (Case 2) on the morphodynamics of the fan–delta system. These operation choices would impact the deltaic morphology and the shoreline migration rate on an engineering time scale.

Table 1 Parameters related to the morphodynamics of the fan–delta system in Wabush Lake

Parameter	Value	Notes
S_s	1470 m	Current condition
$\bar{\theta}_F$	120°	Expanding angle
R	1.95	$R = \rho_s/\rho_w - 1$
λ_p	0.4	Porosity
D_s	0.2 mm	Characteristic grain size
α_r	15	Sand fan
α_s	16.8	Sand fan
τ_a^*	1.8	Sand bed channel
S_a	0.07	Foreset slope
$\eta_{\bar{r}=1}$	0 m	Water level in Wabush Lake
$\eta_{\bar{r}=0}$	30 m	Sediment source point elevation
$\Delta\eta_f$	30 m	Elevation drop on foreset
Q_0	0.14 $m^3\ s^{-1}$	Current tailings production rate
Q_w	3.4 $m^3\ s^{-1}$	Current water supply rate

Table 2 Permanent form solutions

Parameter	Case 0	Case 1	Case 2
Q_0 ($m^3\ s^{-1}$)	0.14	0.28	0.14
Q_w ($m^3\ s^{-1}$)	3.4	3.4	6.8
S_s (m)	1452	719	2921
$\dot{S}_u$ (m $year^{-1}$)	60	222	31

Notes: Q_0 is used to identify the tailings production rate. Q_w is the water supply rate, while S_s is the size of the fan. The fan–delta moves as a whole with a speed $\dot{S}_u$ in the permanent form solutions.

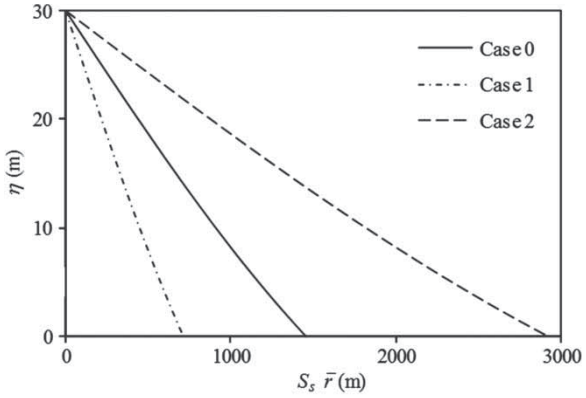

Figure 7 Profiles of permanent form for Case 0, Case 1, and Case 2. The fan elevation shows a similar convex shape

In particular, the permanent form solutions using the parameter sets in Cases 1 and 2 as listed in Table 2 will be compared with those using the current setting in Wabush tailings (Case 0) as listed in Table 1. The other parameters, such as the porosity and characteristic grain size, are kept constant across these three cases. The model equations are solved iteratively until the permanent form solution is reached. Table 2 lists the solutions of the permanent form, including the size of the delta topset and the downstream migration rate of the fan–delta system. The size of the delta topset in Case 0 is similar to the current delta size in Wabush Lake, which indicates that the present fan–delta already reached a steady state. If the sediment and water supply rates are not changing in time, the fan–delta will maintain its current shape and move downstream in the permanent form (as suggested by Fig. 3b).

As the tailings production rate is doubled (Case 1) without changes in the water discharge, the size of the delta surface decreases and the moving speed in the permanent form solution increases. As the water supply rate is doubled (Case 2) with the same sediment discharge than in Case 0, the size of the topset increases and the moving speed decreases. Figure 7 shows the permanent forms of the fan–delta elevation profile for the three cases. Convex-down profiles with different average slopes are observed, which is an important feature of a channelized fluvial system (Parker *et al.* 1998).

5 Application to Wabush tailings: morphodynamic evolution

The previous section studied the permanent form solutions observed first in the laboratory experiments by Fernandez *et al.* (2011). As to reach the permanent form may require time (years), it will be then useful to characterize the fan–delta morphodynamics variations in response to a modification of the operating parameters. This will allow to approximating the fan geometry during the transitional period before reaching the permanent form. Particularly, this work examines the time evolution of the deltaic system (herein Case 0), while it responds to the following two configurations: (a) the tailings production rate is doubled, while the water supply is maintained at the current level (Case A) and (b) the water supply rate is doubled, while the tailings production rate is maintained at the current level (Case B) (Fig. 8). From previous discussion, it is understood that as time progresses, the morphodynamics of fan–delta for Cases A and B will approach to the permanent form of Cases 1 and 2, respectively. In Cases A and B, the initial conditions, that is, the fan–delta elevation profile and the size of the fan, are chosen as the permanent form of Case 0.

Figures 9 and 10 show the moving speed of the sediment source point ($\dot{S}_u$) and the fan–delta growth rate ($\dot{S}_s$) against time for Cases A and B, respectively. In Case A, the sediment source point initially moves at about 10^4 m year^{-1}; then, after the sediment rate is doubled ($t \ll 1$ year), its speed drops in time until $t \sim 1$ year. The fan–delta growth rate shows the same trend: the shrinking rate ($-\dot{S}_s$) starts at a rate of $\sim 10^4$ m year^{-1}, and at $t \sim 1$ year, it drops significantly. By the time $t \sim 2$ years, the fan–delta system is moving forward with a constant speed $\dot{S}_u = 222$ m/year and a fixed size, as expected from the permanent form solution from Case 1. In Case B, the sediment source point initially retreats upstream at a speed $-\dot{S}_u = \sim 10^4$ m year^{-1}, however, the sediment source point ceases to retreat at $t \sim 8$

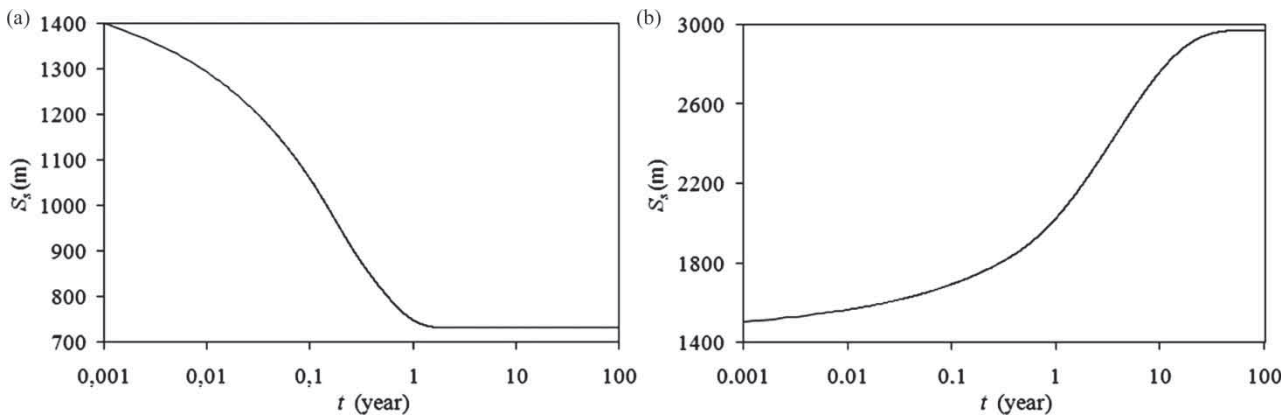

Figure 8 Fan size (S_s) against time for (a) Case A performed with a double-tailing production and (b) Case B performed with a double-water supply

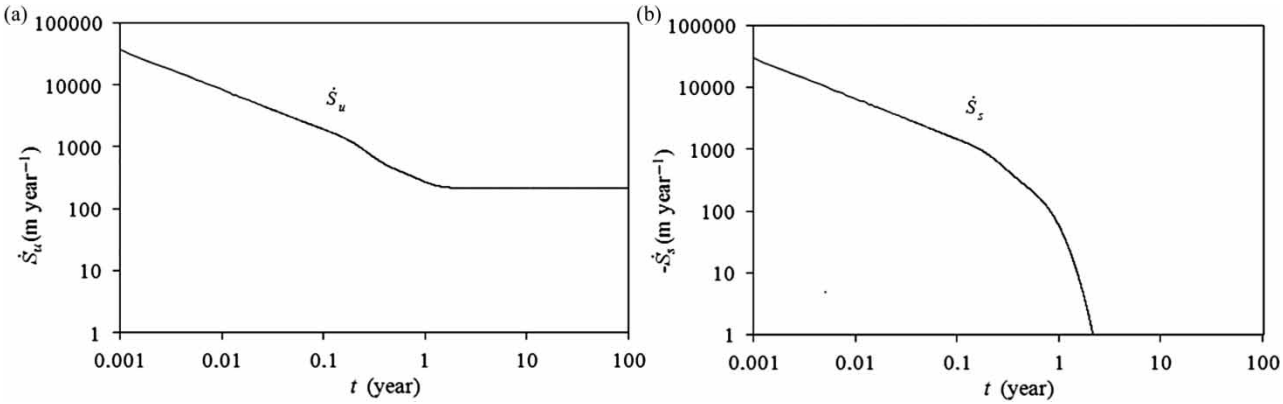

Figure 9 Case A: moving speed of the sediment source point $\dot{S}_u$ and the shrinking rate of the fan $-\dot{S}_s$ over time

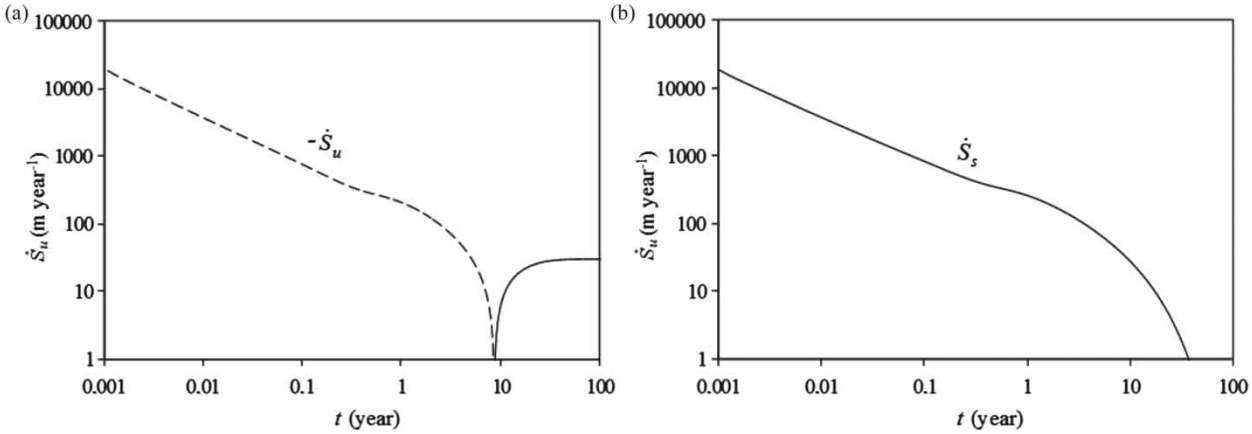

Figure 10 Case B: moving speed of the sediment source point $\dot{S}_u$ and the growth rate of the fan $\dot{S}_s$ over time. The dashed line represents upstream moving source point

years when the retreating speed drops rapidly. Afterwards, the sediment source point moves downstream and its moving speed increases in time over $8 < t < 40$ years. The fan–delta grows in size but the growth rate ($\dot{S}_s$) decreases in time. By the time $t \sim 40$ years, the sediment source point moves at a constant speed $\dot{S}_u = 31\,\mathrm{m\,year^{-1}}$ as predicted by the permanent form solution in Case 2.

6 Conclusions

The axially symmetric delta evolution under the constraint of a moving sediment source at a constant rate is modelled. The fan–delta surface is free to grow or shrink in time and the location of the sediment source is allowed to migrate in the downstream direction.

The numerical results presented in this work, together with the laboratory observations described in Fernandez *et al.* (2011), show that there exists a permanent form solution in which the fan–delta system migrates downstream with a fixed shape and at a constant progradation speed under a flat bathymetry. For the permanent form solutions, the size of the fan is proportional to the water supply rate and inversely proportional to the tailings production rate. The moving speed of the sediment source (and so that, of the fan–delta system) in the permanent form solution is proportional to the tailings production rate and inversely proportional to the water supply rate.

Based on the fact that operating parameters may vary according to management considerations, it was important to predict how the fan system may evolve from its initial geometry, that is, Case 0, when sediment load (Case A) and water inflow (Case B) varied with time. Hence, this work proposed a set of relationships between the discharge conditions and the morphological evolution associated with variations of the operating parameters. Particularly, it was found that the response time of the fan–delta system to the change in water supply rate was larger than the response time to the change in tailings production rate.

Acknowledgements

The participation of G. Parker was made possible by funding from the National Center for Earth-surface Dynamics, a Science and Technology Center funded by the US National Science Foundation (EAR-0120914). The manuscript benefited from comments and suggestions of anonymous referees.

Notation

B_{ac} = width of active channels (m)
C_f = resistance coefficient (–)
d_{50} = mean sediment grain size (m)
g = gravity acceleration (m s^{-2})
h = flow thickness (m)
L_{dep} = deposit length required to hold sediment flowing beyond foreset (m)
q_r = sediment discharge per unit width in the radial direction (m^2 s^{-1})
q_w = water discharge per unit width (m^2 s^{-1})
q_θ = sediment discharge per unit width in the azimuthal direction (m^2 s^{-1})
q_r^* = dimensionless sediment discharge (–)
q_w^* = dimensionless water discharge (–)
Q_0 = total tailing or feed discharge (m^3 s^{-1})
Q_r = total sediment discharge (m^3 s^{-1})
Q_t = total sediment discharge (m^3 s^{-1})
Q_w = total water discharge (m^3 s^{-1})
r = expanding radius (m)
r^2 = correlation coefficient (–)
R = Reynolds number (–)
R = submerged specific gravity of sediment
S = bed slope (–)
S_a = foreset slope (–)
S_b = distance feed point to delta toe (m)
S_s = distance feed point to shoreline (m)
S_u = distance in between coordinate systems (m)
t = time (s)
u = vertex of fan–delta; initial position of sediment source (–)
U = mean streamwise flow velocity (m s^{-1})
X_b = base slope (–)
λ_p = deposit porosity (–)
η = deposit elevation (m)
θ_F = expanding angle of fan–delta (°)
ν = kinematic viscosity (m^2 s^{-1})
τ_b = bed shear stress (Pa)
τ^* = shield dimensionless shear stress (–)

References

Engelund, F., Hansen, E. (1967). *A monograph on sediment transport in alluvial streams*. Teknisk Forlag, Copenhagen.

Fernandez, R., Locat, J., Cauchon-Voyer, G., His-Heng, D., Garcia, M., Parker, G. (2011). Co-evolving topset, foreset and bottomset under the condition of a moving sediment source. Part 1: Laboratory experiments. *J. Hydraulics Res.* 49(1), 42–54.

Garcia, M. (2008). *Sedimentation engineering: Processes, measurements, modelling and practice*. Chapter 3. ASCE Manuals and Reports on Engineering Practice No. 110, p. 1132.

Gerber, T., Pratson, L., Wolinsky, M., Steel, R., Mohr, J., Swenson, J., Paola, C. (2008). Clinoform progradation by turbidity currents: Modelling and experiments. *J. Sediment Res*. 78(3), 1167–1186.

Graf, W.H. (1971). *Hydraulics of sediment transport.* McGraw-Hill, New York.

Hooke, R. LeB., and Rohrer, W.L. (1979). Geometry of alluvial fans: Effect of discharge and sediment size. *Earth Surf. Proc. and Landforms* 4(2), 147–166.

Kim, W., A. Dai, T. Muto, and G. Parker. (2009). Delta progradation driven by an advancing sediment source: Coupled theory and experiment describing the evolution of elongated deltas, *Water Resour. Res.* 45, W06428, doi:10.1029/2008WR007382.

Kostic, S., Parker, G. (2003a). Progradational sand-mud deltas in lakes and reservoirs. Part 1: Theory and numerical modeling. *J. Hydraulic Res*. 41(2), 127–140.

Kostic, S., Parker, G. (2003b). Progradational sand-mud deltas in lakes and reservoirs. Part 2: Experiment and numerical simulation. *J. Hydraulic Res*. 41(2), 141–152.

Locat, J., Parker, G., Garcia, M.H., Cauchon-Voyer, G., Fernandez, R.L., Dai, H., Waratuke, A. (2007). Understanding and prediction tailings accumulation, transport and distribution in Lake Rock. *Technical Report* No. LERN-2007-Rock-05, University of Laval and University of Illinois at Urbana-Champaign.

Parker, G., Paola, C., Whipple, K.X., and Mohrig, D. (1998a). Alluvial fans formed by channelized fluvial and sheet flow, I: Theory. *J. Hydraulic Eng*. 24(10), 985–995.

Parker, G., Paola, C., Whipple, K.X., Mohrig, D., Toro-Escobar, C.M., Halverson, M., Skoglund, T.W. (1998b). Alluvial fans formed by channelized fluvial and sheet flow, II: Application. *J. Hydraulic Eng*. 24(10), 996–1004.

Sun, T., Paola, C., Parker, G. (2002). Fluvial fan deltas: Linking channel processes with large-scale morphodynamics. *Water Resour. Res.* 38(8), 26-1–26-10.

Swenson, J.B., Voller, V.R., Paola, C., Parker, G., Marr, J. (2000). Fluvio-deltaic sedimentation: A generalized Stefan problem. *Eur. J. Appl. Math*. 11(4), 433–452.

Whipple, K.X., Parker, G., Paola, C., Mohrig, D. (1998). Channel dynamics, sediment transport, and the slope of alluvial fans; experimental study. *J. Geology* 106, 677–693.